EFDA–JET–PR(07)34

F. Belli, B. Esposito, D. Marocco, M. Riva, Y. Kaschuck, G. Bonheure
and JET EFDA contributors

A Method for Digital Processing of Pile-up Events in Organic Scintillators

A Method for Digital Processing of Pile-up Events in Organic Scintillators

F. Belli[1], B. Esposito[1], D. Marocco[1], M. Riva[1], Y. Kaschuck[2], G. Bonheure[3]
and JET EFDA contributors*

JET-EFDA, Culham Science Centre, OX14 3DB, Abingdon, UK

[1]Associazione Euratom-ENEA sulla Fusione, C.R. Frascati, C.P. 65, Frascati I-00044, Roma, Italy
[2]TRINITI, Troitsk, Moscow Region, Russian Federation
[3]Laboratory for Plasma Physics, Association "Euratom-Belgian State", Royal Military Academy, Avenue de la Renaissance, 30, B-1000 Brussels, Belgium
** See annex of M.L. Watkins et al, "Overview of JET Results ", (Proc. 21 st IAEA Fusion Energy Conference, Chengdu, China (2006)).*

Preprint of Paper to be submitted for publication in
Nuclear Instruments and Methods in Physics Research Section A

ABSTRACT

Pile-up effects in radiation detectors are events in which two or more pulses overlap. In standard analog electronics *pile-up* events are rejected using a *pile-up* inspector. When digital acquisition techniques are used, the recorded waveforms of *pile-ups* can be elaborated and the contributing *single* pulses reconstructed. A method for the off-line digital processing of *pile-ups* from liquid organic scintillators (NE213) is proposed: *pile-ups* are reduced to *single* pulses and then correctly identified as neutrons (*n)* or gammas (*γ).* An analysis of the errors introduced by the method, depending on the number of fitted samples in the pulses, is given. The method has been applied to data acquired in the mixed *n*-*γ* field of JET deuterium plasma discharges from the NE213 detector in the central line of sight of the neutron profile monitor and the results are described.

1. INTRODUCTION

In nuclear experiments, such as tokamaks, radiation detectors may often reach very high count rates, therefore experiencing a high fraction of *pile-ups*: these are events in which two or more pulses overlap (Figure 1). If not properly recognized, these signals are interpreted as *single* events, with energy equal to the sum of the constituting pulses, with a resulting alteration of the recorded count rates and Pulse Height Spectra (PHS). The usual way of dealing with *pile-ups* in standard analog electronics is to minimize the probability of their occurrence making the detector output signals as short as possible by pulse shaping techniques, then identify and reject them by special hardware settings. Thanks to digital acquisition techniques, the recorded waveforms of *pile-ups* can be now analyzed by deconvolution [1] or fitting methods [2] in order to recover – wherever possible – the original *single* pulse information.

When working with organic scintillators, an additional complication is the fact that *pile-ups* may originate from pulses with different shapes due to different incoming radiation: neutrons (*n*) and gamma rays (*γ*). Actually, this pulse shape difference property is used for *n/γ* discrimination in mixed radiation fields [3].

This work illustrates a method for the digital processing of *pile-ups* from liquid scintillator detectors (NE213) and describes its application to data acquired from the neutron profile monitor in the JET tokamak experiment. It will be shown that the elaboration procedure of the digital data is capable of separating the *pile-ups* in *single* pulses and then correctly identify them as *n* or *γ*.

In Section II an overview of the digital acquisition and elaboration system will be given. In Section III the fitting of *single n* and *γ* pulses acquired with the digital system is described. Section IV contains the details of the *pile-up* resolving method. Finally, in Section V the results of the application of this method to *pile-ups* from JET plasma discharges will be shown.

2. DIGITAL ACQUISITION AND ELABORATION

A digital system has been developed in ENEA-Frascati for acquisition and elaboration of pulses from liquid scintillators, based on an FPGA card (C++ programmed, 200 MSamples/s, 14-bit

resolution) and a LabVIEW^{TM} software devoted to acquisition and pulse analysis [4,5]. The signal from the photomultiplier (PMT) coupled to the scintillator is directly sampled by the hardware in discrete bunches according to a Dynamic Windows Data Acquisition (DWDA) logic [4], that automatically increases the time window depending on the length of the pulse (or overlapping pulses). Each data window may therefore contain one ore more pulses. The elaboration software identifies *single* events (i.e. one pulse in the data window) when the pulse amplitude is larger than a threshold value: in our analysis this was set to 150/8192 (8192 =13 bits) corresponding to ~29mV considering the 14-bit resolution and the ± 1.6V input range of the digital system. If two or more overlapping pulses in the data window are found to exceed the threshold value the window is labeled as *pile-up*. The *n/γ* discrimination is carried out on *single* events by comparing the integral of each pulse in two different time intervals (charge comparison method [4]). The *n* and *γ* count rates together with the PHS (by full integration of each pulse) are subsequently determined.
The off-line *pile-up* resolving method described in this paper (see below Section IV), enables to recover the original shape of the digitally acquired pulses contained in each *pile-up* window. The method is based on an appropriate fitting of the first pulse contained in the window, its subtraction from the rest of the data window and the repetition of such operation until all pulses in the window are resolved. In this way, also events that compose *pile-ups* can be treated as single events and subsequently identified as *n* or *γ*.

3. PULSE FITTING

A database of about 55000 *single* pulses (70% *n*, 30% *γ*) acquired with the digital system described above has been used to test different fitting functions. The database contains pulses from a JET deuterium plasma discharge of the November 2006 experimental campaign (#68495, 0.6 s, about 42000 events, mostly *n* with about 8% of *γ* events, identified by the charge comparison method) and ^{22}Na *γ* calibration source (30s, about 13000 *γ* events). The digital system was connected to the NE213 scintillator (25mm diameter × 10mm thickness) coupled to an EMI9134B PMT (25 mm diameter, 9-stage fast linear focussed) installed in channel #15 of the JET neutron profile monitor [6].

The pulse signal *I(t)* from the PMT can be modeled with enough accuracy using a double exponential with two decay constants, t_f (fast) and t_s (slow), typical of the scintillator material and relative magnitudes A and B different for *n* and *γ* [3]:

$$I(t) = A\exp\left(-\frac{t}{t_f}\right) + B\exp\left(-\frac{t}{t_s}\right) \tag{1}$$

The PMT circuit, as shown in the scheme of Figure 2, introduces another decay constant $\tau = RC$. Solving the equations system for the circuit with the signal I(t)

$$\begin{cases} I(t) = A\exp\left(-\dfrac{t}{t_f}\right) + B\exp\left(-\dfrac{t}{t_s}\right) \\ I(t) = \dfrac{V(t)}{R} + C\dfrac{dV(t)}{dt} \end{cases} \tag{2}$$

the response function is obtained:

$$V(t) = V_0 + A_f\left(\exp\left(-\frac{(t-t_0)}{\tau}\right) - \exp\left(-\frac{(t-t_0)}{t_f}\right)\right) + A_s\left(\exp\left(-\frac{(t-t_0)}{\tau}\right) - \exp\left(-\frac{(t-t_0)}{t_s}\right)\right) \quad (3)$$

where $A_f = \frac{ARt_f}{\tau - t_f}$ and $A_s = \frac{BRt_s}{\tau - t_s}$, $\tau = RC$.

In our case, with R = 50Ω, C ~ 40-100 pF, a value τ between 2ns and 5ns should be obtained. Equation (3) describes the output pulse. Note that, as the analyzed pulses are already baseline-subtracted, $V_0 = 0$.

The pulses have been fitted using Equation (3) by means of the Levenberg-Marquardt method (6 free parameters) and the following decay constant mean values have been obtained: t_{f3} = 5.0 (standard deviation, SD = 0.8) ns; t_{s3} = 40.0 (SD = 14.0) ns. These values agree with those found in literature for the same scintillator [2]. A broad distribution has been found for τ (range 0-5 ns), with a maximum around τ = 4.2 ns: this means that at the sample rate of the digitizer (200 MSamples/s) the shortest decay time is not well discerned, and its value cannot be fixed univocally for the pulse fitting. Therefore, it has been decided to use the simpler two–exponential decay fitting function. In practice, this means to assume, as a first approximation, a linear response function of the PMT circuit of Figure 2 to the scintillator signal (that is neglecting the τ constant):

$$V(t) = A_f \exp\left(-(t-t_0)/t_f\right) + A_s \exp\left(-(t-t_0)/t_s\right) \propto I(t) \quad (4).$$

Fitting the pulses from their peak onwards (4 free parameters, with $t_0 = 0$) with Equation (4), the following decay constant mean values are obtained: t_{f4} = 7.5 (sd = 2.5) ns; t_{s4} = 45.0 (sd = 16.5) ns. The fitting procedure applied separately to *n* and γ has not shown any substantial difference in the obtained values of t_s and t_f. Therefore, in the *pile-up* resolving method (described below in Sections IV and V), the t_{s4} and t_{f4} mean values will be used and the pulses will be fitted with 2 free parameters (A_f and A_s). Applying this procedure to the *single* pulses database, the resulting distribution of the ratio A_f/A_s is shown in Figure 3. Incidentally, note that n/γ discrimination can be obtained through this procedure, but of course, the charge comparison method is more accurate and faster.

4. PILE-UP RESOLVING METHOD

The fitting procedure described in Section III has been used to reconstruct the shapes of pulses overlapped in *pile-ups*. Once the first pulse is reconstructed, it is subtracted from the second pulse and so on. This method is illustrated in Figure 4:

(a) the original *pile-up* data window is cut 3 samples before the second peak (3 samples have been found as the maximum rising time in the most energetic pulses of our pulse database) and the resulting original “good” data corresponding to the first pulse are used to perform

the pulse fit, using the two-exponential decay function described in Section III, starting from the pulse peak sample;

(b) the fitted data are used to complete the "missing" part of the original pulse: a pulse is then obtained as a combination of original and fitted samples, so that as much as possible original data are preserved;

(c) the resulting pulse is subtracted from the original window. This procedure is repeated as many times as the number of peaks detected in the window.

The algorithm used in peak detection is based on a quadratic least squares fit. In order to avoid false peak detection due to noise, the minimum distance between consecutive peaks has been set to 3 sample points: this means that we cannot identify *pile-ups* due to overlapping pulses whose peaks are separated less than 15ns. These events will be therefore recorded and processed as single pulses.

The main questions arising from this pile-up resolving procedure are: 1) which is the error introduced in the calculation of the pulse integral (note that this integral will be used in the PHS)?; 2) which is the minimum number of samples needed to fit a pulse in a sufficiently reliable way? (in other words, how near can be two overlapping pulses in order to be possible to resolve them?). In order to answer these questions we have considered a dataset of about 12190 *single* events ($n + \gamma$) belonging to Pulse No: 69093, for PHS integrals from 0 to 34800 (i.e.: for pulse lengths up to 97 samples).

The average percentage error of the integral as a function of the used fitting points is obtained as follows: the pulses are cut at increasing numbers of samples from their peaks and applying the (a) and (b) steps previously described, the integral of the actual pulse is compared with the integral of the combined (original+fitted) pulse in each case (as illustrated in Figure 5; also shown the standard deviation).

It can be seen that after 7 samples (i.e.: 35ns) the average error in the integrals is already between ±8%. Shortest pulses contribute to such average error just for low values of fitting points, and the average error goes to zero as the number of samples increases.

To compare the quality of our pulse shape fitting using Equation 4 instead of Equation 3, for the same datasets used for Figure 5 the percentage error introduced with a fitting model using Equation 3, with fixed values t_f = 5ns, t_s = 40ns and τ = 4.2ns, was also calculated. Figure 6 shows the results: the relative average error is worse, especially for lower fitting sample values. This, together with a greatly reduced elaboration time, justifies the use of the simplified model of Equation 4.

Figure 7(a) illustrates the peak distance distribution in the *pile-ups* recorded during Pulse No: 69093. The distribution is, as expected, exponential, but only from 250 ns onwards. For lower values the distribution is flat due to the use of the software threshold.

The minimum number of fitting samples for the pulses depends on the maximum error that is required in the integral calculation of the first pulse (see the PHS in Figure 5). As the data window must be cut 3 samples before the second peak (as explained in Section IV), 3 more samples must be added: Figure 7(b), the same of Figure 5 with horizontal scale in ns and shifted by 15 ns (i.e.: 3

samples time), shows the error limits in the PHS spectra as a function of the minimum peak distance chosen to resolve *pile-up* events. Figure 7(c) shows the corresponding percentage of these events resolved from the total of Figure 7(a). For example, if we want to limit our integral error between ±8% we have to use a minimum peak distance equal to 50 ns (i.e.: a minimum of 7 fitting points, corresponding to 35 ns samples length, will be used to reconstruct the pulse shapes); from Figure 7(c) this means that ~87% of the *pile-up* events will be resolved. The remaining events can be used for counting rates purposes, but must be excluded for spectral analysis.

5. APPLICATION OF THE PILE-UP RESOLVING METHOD IN PLASMA DISCHARGE DATA

The *pile-up* resolving method described in Section IV has been applied to the analysis of data acquired with the digital system, connected to the detector of channel #15 of the JET neutron profile monitor [6], during the November 2006 JET experimental campaign. As an example, the results obtained for the highest count rate discharge so far acquired (#69093, Figure 8) are reported in the present section: the acquisition lasted 120 s and includes 40 s of plasma discharge and 80 s of ^{22}Na calibration source.

Data have been analyzed with the standard software (see Section II) and *single* count rates and PHS have been obtained. The events recognized as *pile-ups* have been treated with the *pile-up* resolving method and re-analyzed with the standard software to obtain the *pile-up* count rates and PHS; for this analysis no lower limit on minimum peak distance (see Section IV) in the pile-up events has been set.

In Figure 9 the separation plots for *single* and *pile-ups* events are reported: a total of about 10^6 *single* and ~10^5 *pile–up* events have been recorded and almost all the *pile-up* events have been resolved. Average n/γ ratios equal to 9.3 (SD = 0.8) and 8.7 (SD = 0.9) have been respectively observed for *single* and resolved *pile-up* events during the auxiliary heated phase of the discharge.

A. PULSE HEIGHT SPECTRA

Single and *pile-up* PHS (normalized to their total integral) from *n* and γ have been compared (Figure 10). The two neutron spectra are very close (almost within 15%, shown by the dashed lines) with the exception of very low channel numbers (< channel 13), where in any case the n/γ separation is not optimal; at high channel number (> channel 75) the statistics of the *pile-up* spectrum is too poor for a quantitative comparison, but the deviation between the two spectra does not show any systematic trend. Deviations of the same order are observed in the γ spectra (Figure 11). The channel window used to select pulses produced by 2.5MeV neutrons (*DD* window [7]; channels 23 to 64 corresponding to proton energies 1.8–3.7MeV) and 14.1MeV neutrons (*DT* window, channels >195 corresponding to proton energies >8.5MeV) are also indicated for the neutron spectra: approximately 50% of the counts belong to the *DD* window and 0.2% to the *DT* window both for *single* and resolved *pile-up* neutrons. The chosen software threshold 150/8192 corresponds to ~1MeV proton energy.

B. COUNT RATES

The neutron count rate in the *DD* window obtained by adding the contribution of the resolved *pile-ups* to the *single* count rates ($n_{DD\ true} = n_{DD\ single} + n_{DD\ resolved\ pile\text{-}up}$) has been calculated and is shown in Figure 12.

Typically, if no *pile-up* resolving method were used, the only possibility for correcting the neutron count rate in order to take into account the rejected *pile-up* events, would be to multiply (in each time bin of the neutron rate time vector) the *single* count rate by the factor *C* ($n_{DD\ corrected} = n_{DD\ single} * C$, also shown in Figure 12):

$$C = 1 + \frac{\#\ of\ pile\text{-}up\ pulses}{\#\ of\ single\ pulses} \tag{5}$$

Of course, as this correction does not include any information about the kind and energy of the pile-upped particles (in the case above, for example, the neutron count rate in the *DD* window is corrected considering also *single* and *pile-up* events originating from all γ and those *n* outside the window), a distortion in the count rate may occur. However, $n_{DD\ corrected}$ can give the correct result if *single* and *pile-up* neutron spectra and *single* and *pile-up* γ spectra are (in each time bin) proportional (see Appendix). On the contrary, using the *pile-up* resolving algorithm described in Section IV, it is possible to discriminate between *n* and γ inside *pile-up* events and to calculate their energy; this allows to correctly add their contribution and then to recover the *true* count rate in any particular energy window.

For the case of Figure 12 (Pulse No: 69093), considering that *single* and *pile-up* neutron spectra and *single* and *pile-up* γ spectra (even though integrated in the whole discharge) are very close in shape, and that *single* and *pile-up* n/γ ratios are also very close, the overall agreement between the neutron time traces detrmined using the two above methods ($n_{DD\ true}$ and $n_{DD\ corrected}$) is, as expected, good: the difference between the count rates is always below 1% and the mean percentage difference is ~0.2% (SD ~0.3%) as shown in Figure 12. Actually, since the observed n/γ ratio is ~9, the contribution of γ to the correction factor *C* is small, and the differences between $n_{DD\ corrected}$ and $n_{DD\ true}$ are mainly influenced by the relation between the values that the ratio *n(p)/n(s)* (see Appendix) assumes inside the window and in the full spectrum.

If the *single/pile-up* proportionality in the pulse height spectra is altered a systematic difference is instead visible between *true* and *corrected* count rates. Two cases will be discussed:

a) The normalized *n* and γ spectra of *single* and resolved *pile-up* events are shown in Figures 13 and 14 for the same discharge previously analyzed (Pulse No: 69093), here re-elaborated using a lower threshold for peak detection (40/8192 instead of 150/8192, anyway higher than the intrinsic noise of the acquisition system). The lowering of the threshold produces:

- Addition of a high number of low energy pulses to *single n* and γ spectra: *single* pulses with 40<peak<150;
- Removal of pulses from the *single* spectra: pulses formed by one event with peak>150 pile-upped with pulses having 40<peak<150;

- Addition of both low and high energy pulses to the *pile-up* spectra: pile-upped low energy pulses with 40<peak<150 and the events of previous point.

Spectral differences are mainly visible in the *n* spectra, and particularly in the high-energy region: the longer tail of *n* pulses with respect to γ pulses increases their *pile-up* probability. Since in this case the *n(p)/n(s)* ratio in the *DD* window is lower than its average value in the full spectrum, we expect $n_{DD\ true}$ to be lower than $n_{DD\ corrected}$. A small (~1%) but systematic difference is indeed observed with $n_{DD\ true} < n_{DD\ corrected}$ (Figure 14).

b) The neutron count rates in the DT energy window ($n_{DT\ true}$ and $n_{DT\ corrected}$) have been compared (threshold set to 40/8192). A much higher difference than in the previous example is found: the average is about 50% and $n_{DT\ true} > n_{DT\ corrected}$ (see Figure 15). In this case, the difference can be attributed to the fact that the *n(p)/n(s)* ratio in the *DT* window it is higher than its average value on the full spectrum. A similar trend, but with average difference ~5% is also observed for DT neutron count rates obtained setting the threshold to 150/8192.

CONCLUSIONS

A method for the off-line digital processing of *pile-ups* from organic scintillators (NE213) has been described: the method is based on a recursive procedure of fitting and subtraction of the superimposed pulses that compose a *pile-up* event.

The *pile-up* resolving procedure has been applied to data acquired in the mixed *n*-*γ* field of JET deuterium discharges with the NE213 detector of the central line of sight of the neutron profile monitor connected to a 14-bit 200 MSamples/s digital acquisition system. The results indicate that a simple double exponential function (with no additional decay constant due to the PMT circuit) is appropriate for pulse fitting; moreover, the error introduced by the fitting can be kept below 10% if the resolving procedure is applied only to *pile-ups* with successive peaks separated by more than 50 ns. In these conditions ~87% of the *pile-up* events can be resolved and used for spectral analysis; the remaining events can be used for counting rates purposes only. It can be expected that in principle this procedure can work up to a maximum count rate of roughly 20 MHz (i.e.: ~1/50 ns).

The *n* and *γ* spectra of the resolved *pile-ups* have been evaluated for a high count rate JET discharge at two different values of the peak detection threshold. The neutron count rates in DD and DT energy windows obtained adding to *single* neutrons the contribution of neutrons originated from resolved *pile-ups* (*true* count rate) have been calculated (for the two threshold values) and compared with those obtained using a simple *pile-up* correction factor that only includes the number of *pile-up* events (*corrected* count rate). Higher differences have been found between *DT true* and *corrected* count rates (~50% in the low threshold case and ~5% in the high threshold case) while DD count rates show lower discrepancies (1% in the low threshold case). Such diffferences can be explained in terms of differences between *single* and resolved *pile-up n* and *γ* spectra.

ACKNOWLEDGMENTS

This work has been partly funded by EFDA Underlying Technology Task ENEA_UT06_TPD_PDS and EFDA-JET Task JW5-EP-SEN-SP3 (Small Enhancement for Neutronics).

REFERENCES

[1]. W. Guo et al., Nucl. Instr. and Meth. **A544** (2005) 668

[2]. S. Marrone et al., Nucl. Instr. and Meth. **A490** (2002) 299

[3]. H. Klein, Radiation Protection Dosimetry **107** (2003) 95

[4]. D. Marocco et al., International Workshop on Fast Neutron Detectors and Applications (Cape Town, April 2006), PoS (FNDA2006)028, http://pos.sissa.it/

[5]. B. Esposito et al., Nucl. Instr. and Meth. **A572** (2007) 355

[6]. J.M. Adams et al., Nucl. Instr. and Meth. **A329** (1993) 277

[7]. O.N. Jarvis, Plasma Phys. Control. Fusion **36** (1994) 209

APPENDIX

In each time bin the *true* factor to be used for the correction of *single* neutron counts in a given energy window (*w*) is:

$$C_{true} = 1 + \frac{n_w(p)}{n_w(s)}$$

where $n_w\,(p)$ and $n_w\,(s)$ respectively indicates the in-window *pile-up* and *single* neutrons occurred during the time bin. The simple correction factor *C* is instead

$$C = 1 + \frac{n_{total}(p) + \gamma_{total}(p)}{n_{total}(s) + \gamma_{total}(s)}$$

If *single* and *pile-up* spectra are proportional, i.e. if

$$n_{total}(p) = k\, n_{total}(s)$$
$$\gamma_{total}(p) = k\, \gamma_{total}(s)$$

single and *pile-up* events share the same n/γ ratio (*R*) and then

$$C = 1 + \frac{n_{total}(p)\left(1 + 1/R\right)}{n_{total}(s)\left(1 + 1/R\right)} = 1 + \frac{n_{total}(p)}{n_{total}(s)} = 1 + \frac{n_w(p) + n_{rest}(p)}{n_w(s) + n_{rest}(s)}$$

where the subscript *rest* indicates the counts originating from pulses outside the window. Moreover, if proportionality holds, the ratio between out-of-window and in-window counts (*h*) is the same for *single* and *pile-up* neutrons and then

$$C = 1 + \frac{n_w(p)\left(1 + h\right)}{n_w(s)\left(1 + h\right)} = 1 + \frac{n_w(p)}{n_w(s)} = C_{True}$$

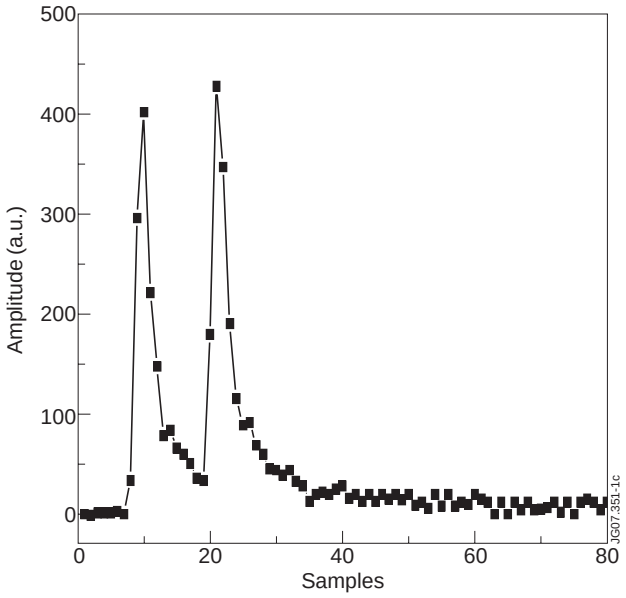

Figure 1: Typical pile-up event.

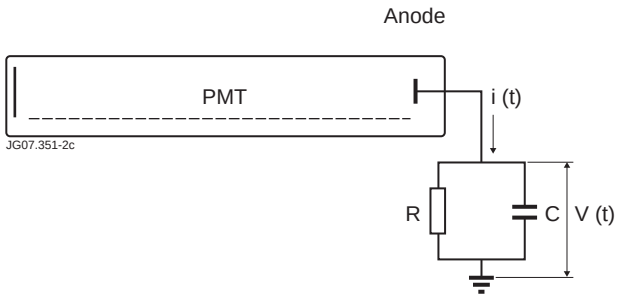

Figure 2: Scheme of the PMT circuit.

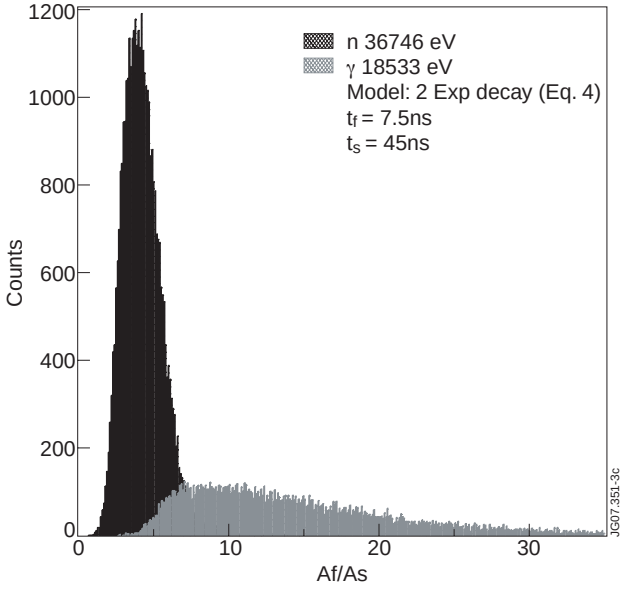

Figure 3: A_f/A_s distributions for n (black) and γ (gray) signals fitted with Equation (4).

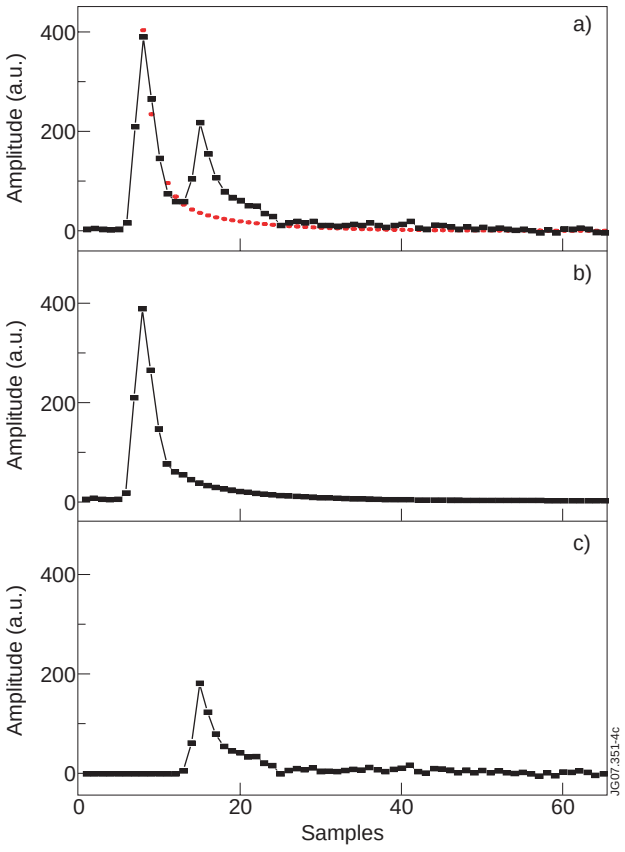

Figure 4: Pile-up data processing. a) Pile-up data and fit of first pulse b) Combined first pulse (original + fit) c) Second pulse after subtraction of combined first pulse

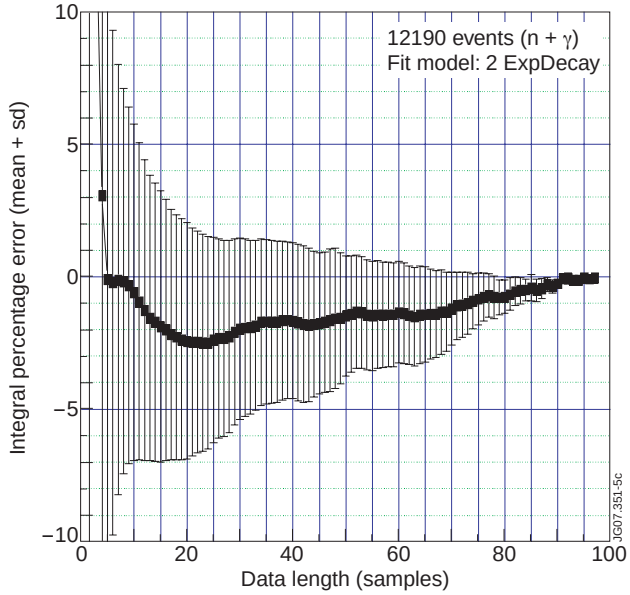

Figure 5: Percentage error introduced in the calculation of integrals using the pile-up resolving method as a function of the number of samples used for fitting (the fitting model of this dataset is Equation (4)).

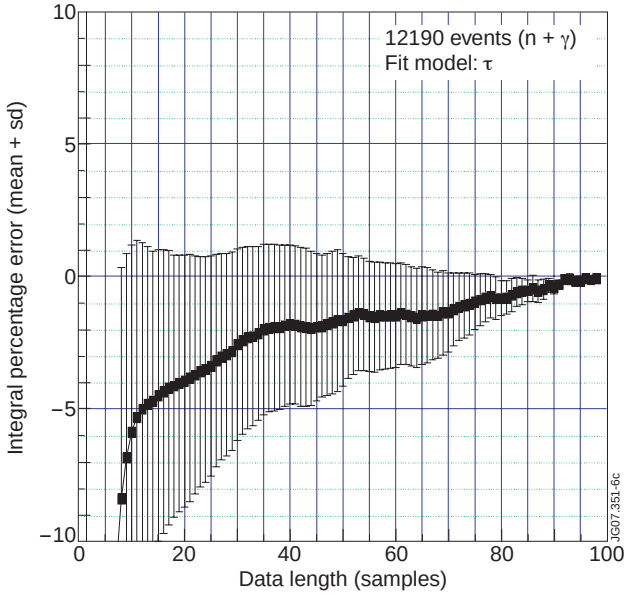

Figure 6: The same dataset of Figure 5 fitted using Equation (3)

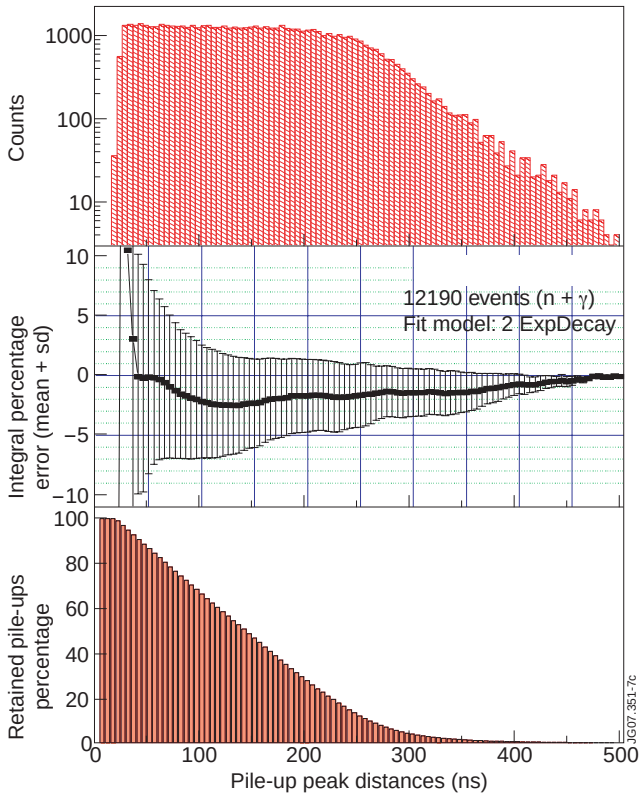

Figure 7: Distribution of the pile-up peak distances (top), the corresponding integral percentage error (mean + standard deviation) of the resolved pulses (middle) and the corresponding percentage of resolved pile-up events (bottom).

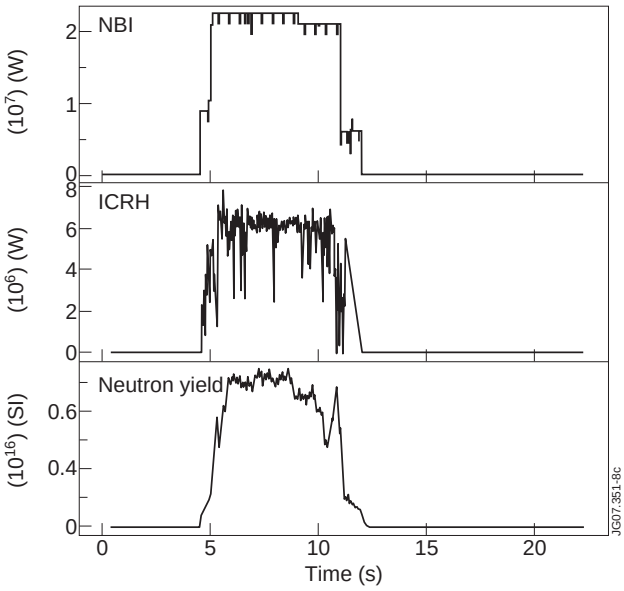

Figure 8: JET Pulse No: 69093: neutron yields measured by JET neutron monitors (fission chambers) and time traces of the applied auxiliary heating; (NBI: neutral beam injection, ICRH: ion cyclotron resonance heating).

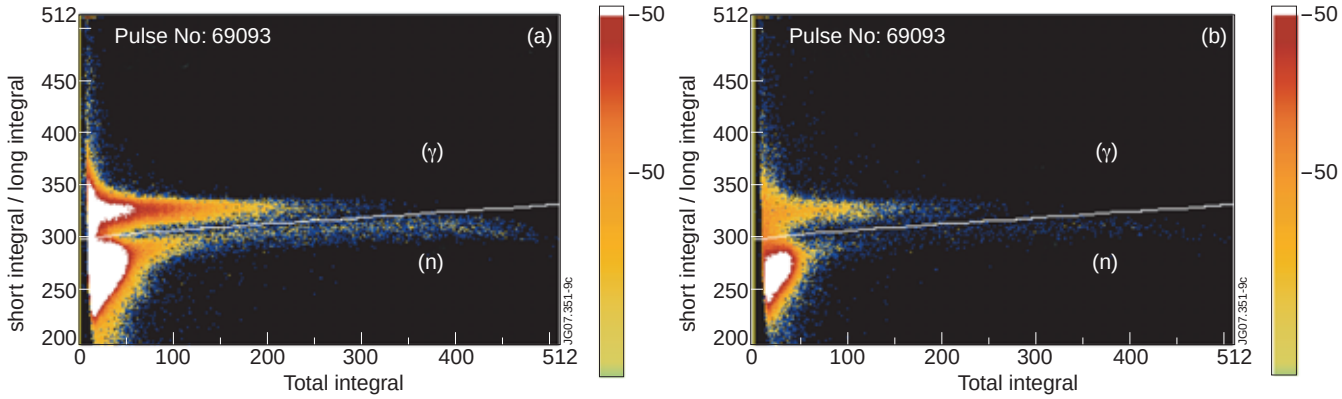

Figure 9: JET Pulse No:69093: n/γ separation plots for single (a) and resolved pile-up (b) pulses. x axis= total integral (i.e. energy) of the pulse; y axis= ratio between short and long integral [4,5]; color scale proportional to the number of counts; white line =n/γ separation line.

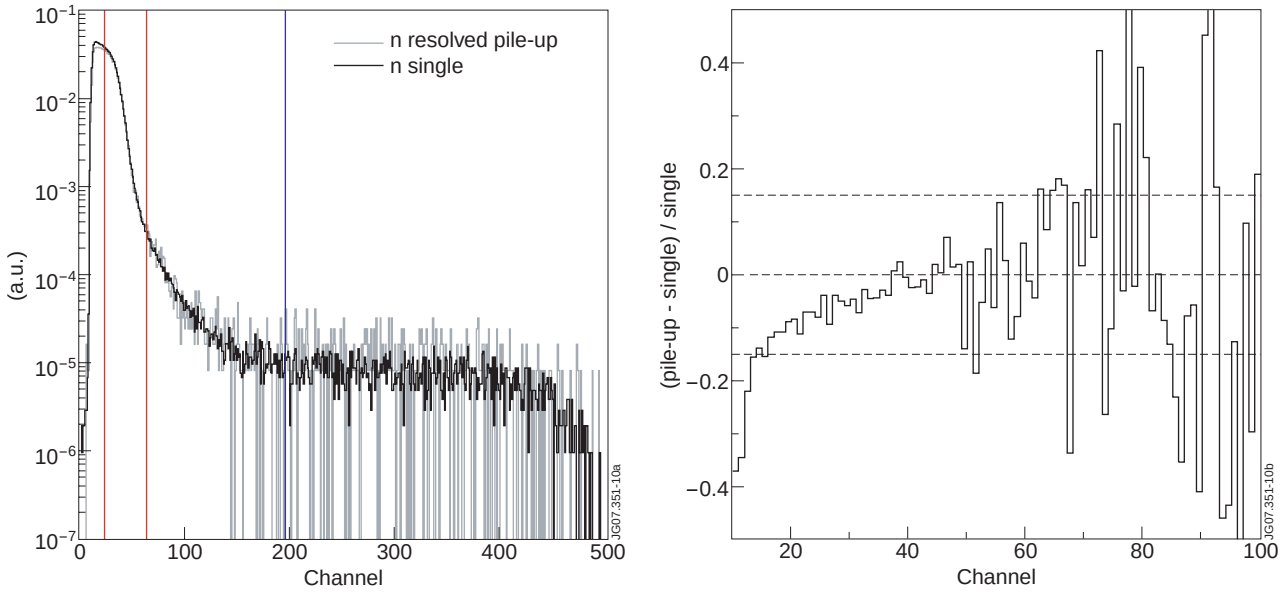

Figure 10: (left) Single neutron spectrum and resolved pile-up *neutron spectrum for Pulse No: 69093 obtained with threshold 150 (red lines=*DD *energy window; blue line=lower limit of the* DT *energy window); (right) deviation between* single *and resolved* pile-up *neutron spectra.*

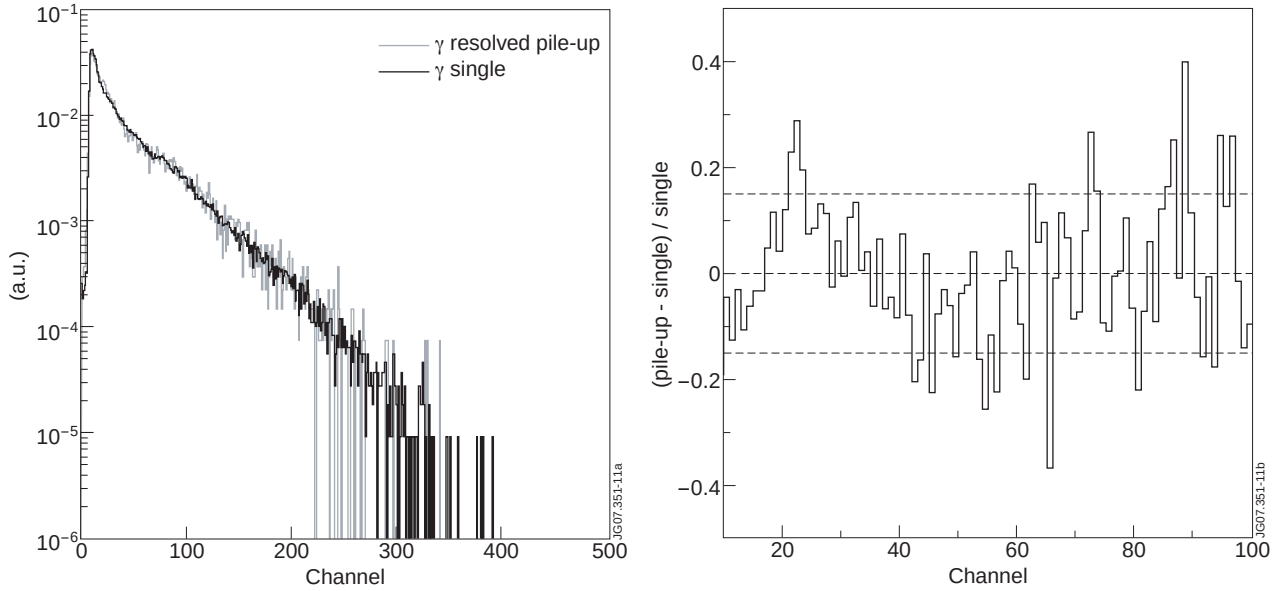

Figure 11: (left) Single γ spectrum and resolved pile-up γ spectrum for Pulse No: 69093; (right) Deviation between single and resolved pile-up γ spectra.

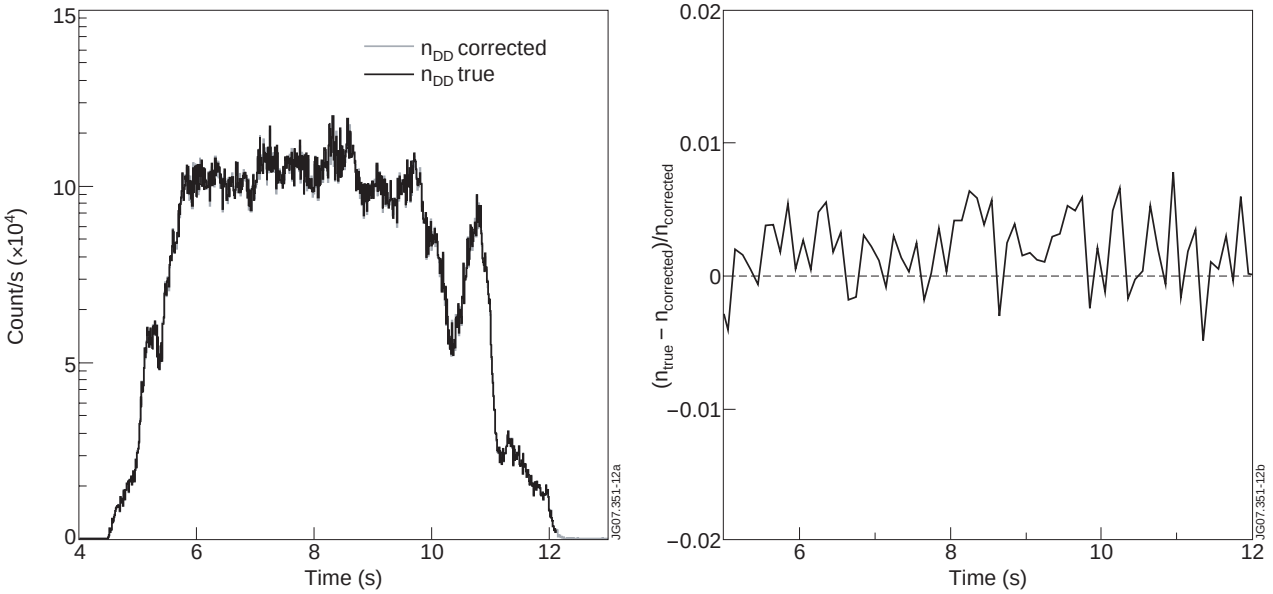

Figure 12: Pulse No: 69093: (left) $n_{DD\ true}$ and $n_{DD\ corrected}$ (10ms time bin); (right) deviation between $n_{DD\ true}$ and $n_{DD\ corrected}$ (100ms time bin).

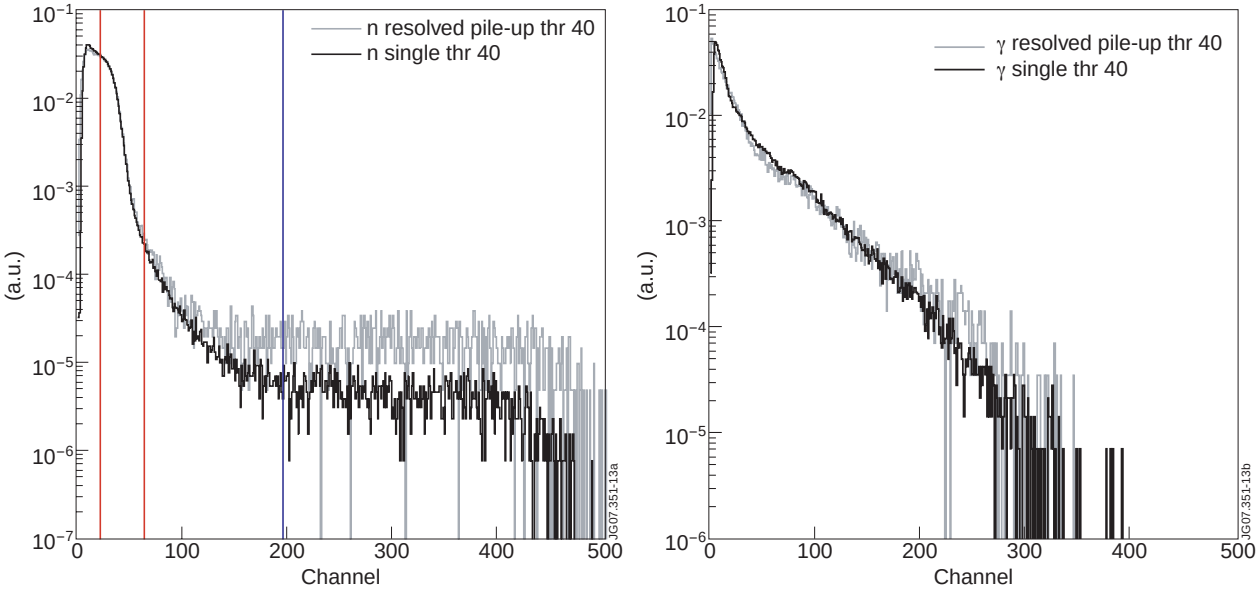

Figure 13: Pulse No: 69093: normalized neutron (left) and γ (right) spectra of single and resolved pile-up pulses obtained with threshold 40/8192 (red lines=DD energy window; blue line=lower limit of the DT energy window).

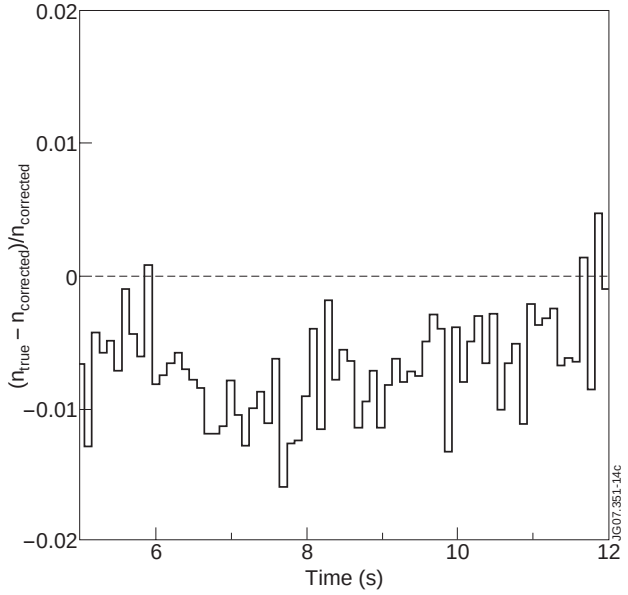

Figure 14: Pulse No: 9093: deviation between $n_{DD\ true}$ and $n_{DD\ corrected}$ obtained with threshold 40/8192 (100 ms average).

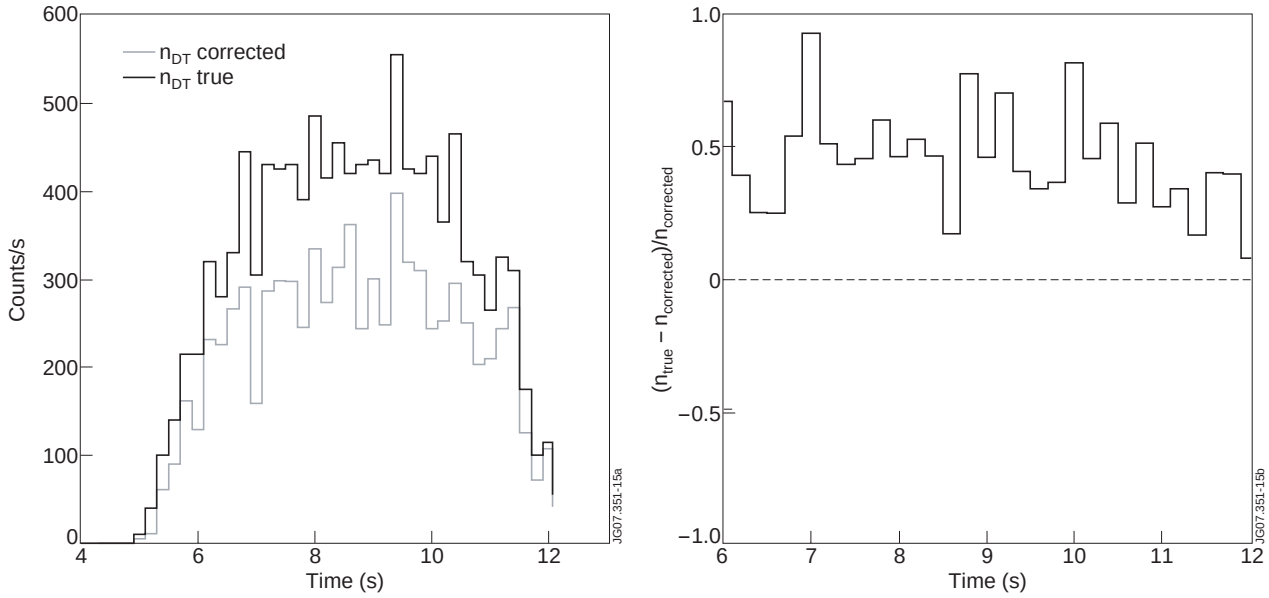

Figure 15: Pulse No: 69093: (left) $n_{DT\ true}$ and $n_{DT\ corrected}$ (threshold 40/8192, 200ms average); (right) deviation between $n_{DT\ true}$ and $n_{DT\ corrected}$.